CHAPTER 12

Rigid Pavement Design

12.1 CALIBRATED MECHANISTIC DESIGN PROCEDURE

As with flexible pavements, the calibrated mechanistic design procedure involves the application of structural models to calculate pavement responses, the development of distress models to predict pavement distress from structural responses, and the calibration of the predicted distress with the observed distress on in-service pavements. Figure 12.1 shows the general methodology for rigid pavement design. This figure is similar to Figure 11.1 for flexible pavements, except for step 5 on structural models and step 8 on distress models.

The structural models for rigid pavement analysis are more advanced than the distress models. Several finite element programs can be used as structural models, but most of the distress models are regression equations derived empirically with a large scatter of data. The major types of distress to be modeled include fatigue cracking, pumping, faulting, and joint deterioration for jointed concrete pavements and punchouts for continuous reinforced concrete pavements. Some steps in Figure 12.1 are described in Sections 11.1.1 and 11.1.2; only the steps involving these new models are discussed in this section. Most of the models presented herein were developed by the University of Illinois and described in Report 1-26 (NCHRP, 1990).

12.1.1 Structural Models

To analyze rigid pavement systems accurately, Report 1-26 (NCHRP, 1990) indicated that the structural models used must have the following minimum capabilities:

1. To analyze slabs of any arbitrary dimensions.
2. To analyze systems with two layers (slab and subbase), either bonded or unbonded, with the same or different material properties.
3. To analyze slab systems on either a liquid or a solid subgrade.

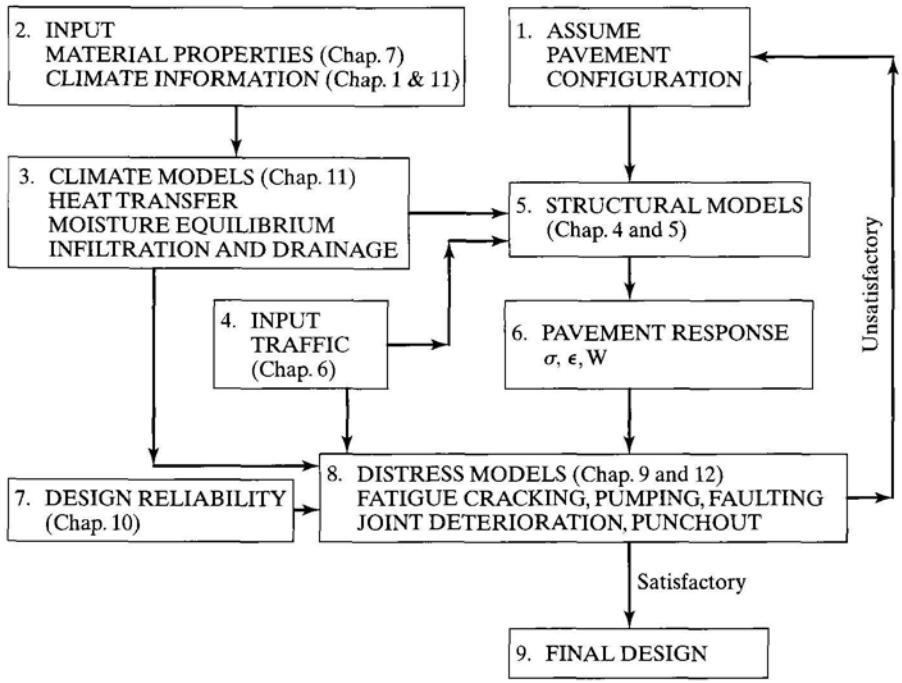

FIGURE 12.1

Methodology of calibrated mechanistic procedure for rigid pavement design.

4. To analyze slab systems with either uniform or nonuniform support, so that loss of support due to erosion or other causes can be taken into account.
5. To analyze multiple slabs with load transfer across the joints or cracks.
6. To consider slab warping and curling simultaneously with load responses.
7. To analyze slabs with variable crack spacings for CRCP design.
8. To analyze slabs with any arbitrary loading conditions, including single or multiple wheels, variable tire pressures, and loads applied at arbitrary assigned distances from cracks, joints, or slab edges.
9. To analyze pavement systems with arbitrary shoulder conditions, including asphalt shoulders, tied concrete shoulders, and extended driving lanes with asphalt or concrete shoulders beyond the extended slab.
10. To analyze systems with nonuniform slab or shoulder thicknesses.

After reviewing several finite element models, Report 1-26 recommended the use of ILLI-SLAB as the basic model for the analysis of rigid pavements. The KENSLABS program presented in this book also meets all the preceding requirements. In addition to liquid and solid foundations, KENSLABS can be applied to a layer subgrade consisting of up to six layers.

Report 1-26 also indicated that the finite element programs require a large computer core capacity, and conventional personal computers with a core capacity of 640 K

are not adequate to obtain reliable and accurate results. This statement was true at the time of the report. With the recent advance in personal computers and the introduction of the Windows operating system, core capacity is no longer a problem. However, a large finite-element program still requires a considerable time to run.

One way to reduce the computer time needed is to develop algorithms or regression equations to replace structural models for calculating pavement responses (Zollinger and Barenberg, 1989). These algorithms can be developed by running a finite element program thousands of times and fitting the results with regression equations. Tabulated values of the regression coefficients can be provided on a disk; the algorithms can be run on a PC. However, this method can be used only for typical designs with a limited number of variables that can be changed, such as PCC thickness, modulus of subgrade reaction, magnitude of single-axle load, and concrete modulus of elasticity. For unusual situations, such as axle loads with special configurations, voids under the slabs, two layers of slabs, and slabs of nonuniform thickness, the finite-element program must still be used.

12.1.2 Fatigue Cracking Models

The fatigue of PCC was described in Section 7.3.2. As with flexible pavements, the accumulation of fatigue damage can be expressed as a summation of damage ratios, defined as the ratio between predicted and allowable number of load repetitions. However, instead of relating to tensile strain, the allowable number of load repetitions is related to the stress ratio, which is the ratio between the flexural stress and the modulus of rupture. The same probability concept used to define percent area cracked can be used to define percent of slabs cracked.

Truck Load Placement The fatigue of concrete can cause both transverse cracking, which initiates at the pavement edge midway between transverse joints, and longitudinal cracking, which initiates in the wheelpaths at transverse joints, usually at the wheelpath nearest the slab centerline. Figure 12.2 shows the most critical loading and stress locations to be considered for fatigue analysis. Transverse cracking is caused by the midslab edge loading, and longitudinal cracking is caused by the joint loading.

The lateral distribution of traffic means that wheel loads are not applied at the same location, so only a fraction of the load repetitions need be considered for fatigue damage. Report 1-26 suggested the use of an equivalent damage ratio, EDR, for each critical loading position. EDR is the ratio of the traffic applied at a critical location that

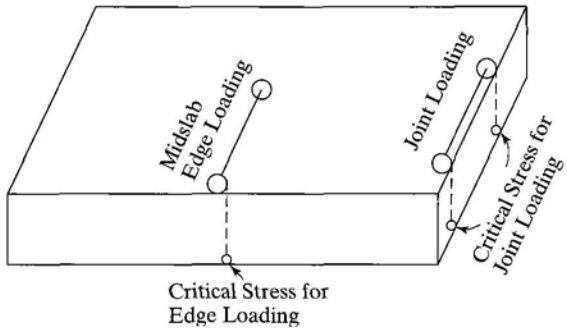

FIGURE 12.2
Critical loading and stress locations for fatigue analysis.

will produce the same accumulated fatigue damage as the total traffic distributed over all locations. It was demonstrated in Report 1-26 that an EDR of 0.05 to 0.06 can be used for the midslab edge loading with asphalt shoulders and that an EDR of 0.25 to 0.28 can be used for joint loading. For edge loading with tied concrete shoulders, the EDR ranges from 0.12 to 0.34. Therefore, the truck-load placement, which is not a factor in flexible pavement design, must be carefully considered in rigid pavement design.

Curling Stress Report 1-26 suggested the use of combined loading and curling stresses for determining the stress ratio and thus the allowable number of load repetitions. In addition to the number of periods and load groups, a new loop indicating curling conditions must be added to Eq. 3.19:

$$D_r = \sum_{i=1}^{p} \sum_{k=1}^{3} \sum_{j=1}^{m} \frac{n_{i,k,j}}{N_{i,k,j}} \tag{12.1}$$

In this equation, D_r is the accumulated damage ratio over the design period at the critical location, i is the counter for periods or subgrade support values, p is the total number of periods, k is the counter for three curing conditions (day, night, and zero temperature gradient), j is the counter for load groups, m is the total number of load groups, $n_{i,k,j}$ is the predicted number of load repetitions for the jth load group, kth curling condition, and ith period, and $N_{i,k,j}$ is the allowable number of load repetitions for the jth load group, kth curling condition, and ith period. The inclusion of curling stress complicates the computation, because the traffic has to be divided into three time periods, each with a different temperature gradient. It does not appear reasonable to combine loading and temperature stresses, since they do not occur at the same frequency. A pavement may be subject to thousands of load repetitions per day due to traffic, but the number of repetitions due to temperature curling is mostly only one a day. If curling stresses cannot be ignored and longer panel lengths have significant effects on fatigue cracking because of higher curling stresses, it is more reasonable to consider the damage ratios due to loading and curling separately and then combined, as illustrated by the Shahin–McCullough model for flexible pavements presented in Section 11.1.4.

Curling may not affect the fatigue life significantly because the curling stress may be subtracted from or added to the loading stress, thus neutralizing the effect. The edge stress is further reduced by moisture warping because the moisture contents at the bottom of slab are very frequently higher than those at the top. The curling stress should be much reduced when new pavements are to be constructed with reasonably short panel lengths. The calibration of the model can further minimize the effect of curling stress. For example, Figure 12.3 shows a plot of calibrated performance curves for jointed concrete pavements relating the percent slabs cracked to the accumulated damage ratio. The stress ratio used in calculating the fatigue relationships shown in the figure included both loading and curling stresses. If curling stresses were eliminated from this calculation, different performance curves would be obtained. However, the percent slabs cracked should not be significantly affected if the same procedure, either including or excluding the curling stress, is used in both design and calibration processes.

The performance curves shown in Figure 12.3 were based on field calibration. For 50% reliability, the theoretical percent slabs cracked at a damage ratio of 1 should be

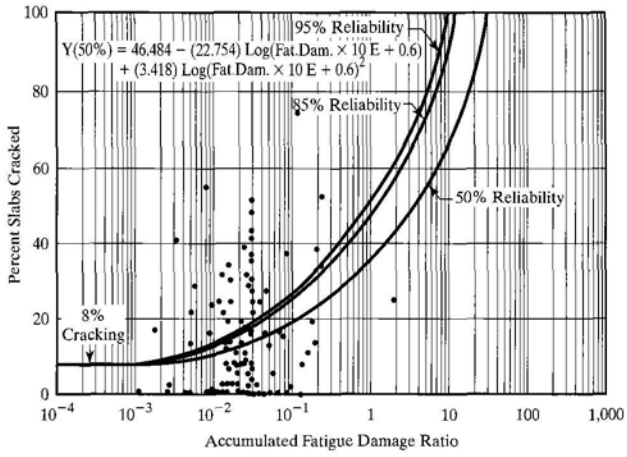

FIGURE 12.3
Calibrated performance curves based on Illinois COPES data. (After NCHRP (1990).)

50%, but the percentage shown in the figure is only 27%. One possible cause for the discrepancy is the difficulty of determining the concrete modulus of rupture during the entire evaluation period from the initial loading to the time of evaluation. Additional research needs to be done on the best method for estimating concrete strength in existing pavements and on how the observed cracking can be correlated with the damage ratio and the probability of cracking.

12.1.3 Pumping and Erosion Models

There is an important mode of distress in addition to fatigue cracking that needs to be addressed in the design of rigid pavements. This is the pumping and erosion of material beneath and beside the slab. In fact, most of the failures in the Maryland and AASHO road tests were the result of pumping.

Factors that influence pumping and erosion include the presence of water, the rate at which water is ejected under the slab, the erodibility of the subbase material, the magnitude and number of repeated loads, and the amount of deflection. No mechanistic models currently available take all of the above factors into account. The only available model is the one developed by PCA, which is described in Section 12.2. The PCA model was based primarily on the results of the AASHO Road Test, and only the corner deflection was taken directly into consideration. Because the subbase materials used in the AASHO Road Test are highly erodible and are currently not used by any of the highway agencies, the application of the model appears to be limited.

Attempts have been made to correlate erosion with rate of water ejection, traffic loads, and pavement deflection through an energy model (Dempsey, 1983; Phu *et al.*, 1986). The thrust of this approach is to calculate the amount of energy involved in the deflection of a pavement system and establish a correlation between the total energy absorbed for given levels of traffic and erosion. These attempts have been moderately successful for specified conditions, but there are other factors affecting erodibility that have not been duly considered. Additional work is needed before these models can be incorporated into a mechanistic-based pavement design procedure.

Report 1-26 also presented an empirically based pumping model that considers all factors believed to influence erosion and pumping of rigid pavements. The model, which can be applied to both JPCP and JRCP by including the type of load transfer as a variable, was developed by using nonlinear regression techniques from a data base of 927 pavement sections from seven states in every continental climatic zone. Because some of the regression constants in the model do not appear reasonable, the model is not presented here. Instead, the COPES pumping models (Darter *et al.*, 1985), which include separate equations for JPCP and JRCP, are presented below. Note that the erodibility of the base course, which is an important factor contributing to pumping and was considered in Report 1-26, was not included in the COPES models.

Jointed Plain Concrete Pavements

$$\text{PI} = (N_{18})^{0.443}[-1.479 + 0.255(1 - S) + 0.0605(P)^{0.5} + 52.65(H)^{-1.747} + 0.0002269(\text{FI})^{1.205}] \quad (12.2a)$$

Statistics: $R^2 = 0.68$, SEE = 0.42, $n = 289$

Here,

PI = pumping index rated on a scale of 0 to 3: 0 for no pumping, 1 for low-severity pumping, 2 for medium-severity pumping, 3 for high-severity pumping
N_{18} = number of equivalent 18-kip single-axle loads, in millions
S = soil type based on AASHTO classification: 0 for coarse-grained soils (A-1 to A-3), 1 for fine-grained soils (A-4 to A-7)
P = annual precipitation, in cm
H = slab thickness, in inches
FI = freezing index, in degree days

Jointed Reinforced Concrete Pavements

$$\text{PI} = (N_{18})^{0.670}[-22.82 + 26{,}102.2(H)^{-5.0} - 0.129(D) - 0.118(S) + 13.224(P)^{0.0395} + 6.834(\text{FI} + 1)^{0.00805} \quad (12.2b)$$

Statistics: $R^2 = 0.57$, SEE = 0.52, $n = 481$

Here, D is the indicator for the presence of subdrainage systems: 0 for no subdrainage system, 1 for subdrainage system.

A pumping prediction model was developed by Purdue University and incorporated in the PEARDARP computer program (Van Wiji, 1985; Van Wiji *et al.*, 1989). The model is based on field data from different sources and on the amount of deformation

energy in the pavement structure. The volume of pumped material is calculated as a function of the deformation energy produced by traffic. This volume is then adjusted to take into account the variations in subbase type, drainage conditions, load-transfer adequacy, subgrade conditions, and climate. The model can be used in the optimum design of rigid pavements by predicting the effect of different design alternatives on the development of pumping. As is true with any regression model, this model is valid only within the data base from which it was derived. It is hoped that more mechanistic-based models can be developed to replace the regression models.

12.1.4 Faulting Models

Faulting at transverse joints is a serious problem that can lead to severe roughness in jointed concrete pavements. The mechanisms of faulting distress in doweled pavements are quite different from those in undoweled pavements. Therefore, these two pavements are discussed separately.

Doweled Pavements Faulting of doweled pavements is caused by the erosion of concrete around the dowels under repeated loading. Because the design of dowels is based on the bearing stress between dowel and concrete, as described in Section 4.4.1, it is natural to assume that faulting is due to excessive bearing stress. It was found that, if the bearing stress is kept below approximately 1500 psi (10.4 MPa), faulting can be limited to an acceptable level.

The maximum bearing stress on dowel bars can be obtained directly by the finite-element computer programs. As an alternative, Report 1-26 recommended the use of Eq. 4.45 to compute the bearing stress. The procedure is the same as the one described in Example 4.12, Section 4.4.1, except that the load is distributed over an effective length of 1.0ℓ, instead of 1.8ℓ, and the load transferred through the joint is assumed to be $0.45W$ instead of $0.5W$, where W is the total load. Using the preceding method to calculate the bearing stress and assuming a modulus of dowel support K of 1.5×10^6 psi (10.4 GPa), the following regression equation based on 280 pavement sections in the COPES data base was obtained:

$$F = (N_{18})^{0.5377}\,[2.2073 + 0.002171(S)^{0.4918} + 0.0003292(\mathrm{JS})^{1.0793} - 2.1397(k)^{0.01305}] \tag{12.3}$$

In this equation,

F = pavement faulting, in inches
N_{18} = number of equivalent 18-kip single-axle loads, in millions
S = maximum bearing stress, in psi
JS = transverse joint spacing, in ft
k = estimated modulus of subgrade reaction on the top of the subbase, in pci

Several climatic variables, such as the precipitation and freezing indexes, were introduced originally but did not show any statistical significance and, therefore, were not included in the model. This is probably due to the limited number of climatic zones in the data base. Because of insufficient data, many other variables, such as permeable

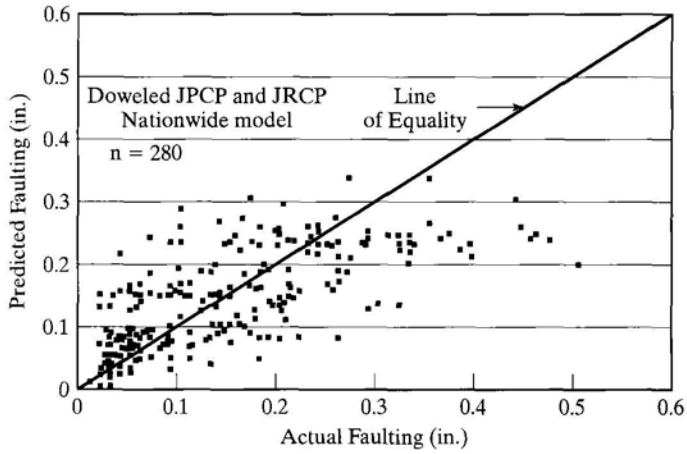

FIGURE 12.4

Predicted faulting versus observed faulting for doweled pavements (1 in. = 25.4 mm). (After NCHRP (1990).)

base, subgrade type, edge support, and sub-drainage are not included. This model must not be used to predict faulting by extrapolation beyond the data range used in its generation. This is particularly true for open-graded drainable bases, which were not included. Figure 12.4 is a plot of predicted faulting versus actual faulting for these 280 sections of doweled pavements. Note that Eq. 12.3 is quite different from Eq. 9.54*a*, which is a later model with a more extended data base and considers the effect of drainage condition, edge support, and soil type.

Figure 12.5 shows the effect of bearing stress on faulting, as obtained from Eq. 12.3, based on N_{18} = 10 million. Two different joint spacings and subgrade moduli

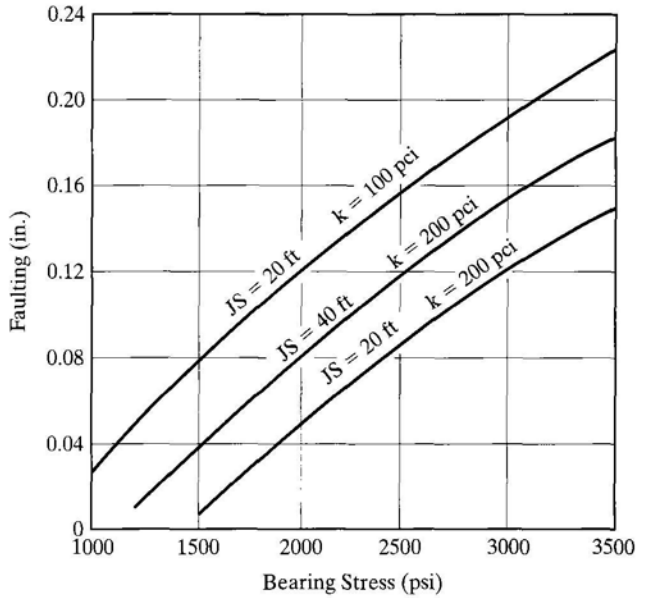

FIGURE 12.5

Effect of bearing stress on faulting. (1 in. = 25.4 mm, 1 ft = 0.305 m, 1 psi = 6.9 kPa, 1 pci = 271.3 kN/m^3).

were used. It can be seen that bearing stress has the most significant effect on faulting and joint spacing the least effect.

Undoweled Pavements To date, no mechanistic-based analyses have been attempted for undoweled pavements. The following regression equation was derived from 186 pavement sections in the COPES data base and presented in Report 1-26:

$$F = (N_{18})^{0.3157}[0.4531 + 0.3367(z)^{0.3322} - 0.5376(100w)^{-0.008437} + 0.0009092(\text{FI})^{0.5998} + 0.004654(B) - 0.03608(\text{ES}) - 0.01087(S) - 0.009467(D)] \quad (12.4)$$

Here,

F = faulting, in inches
N_{18} = number of equivalent 18-kip single-axle loads, in millions
z = joint opening, in inches, which can be determined from Eq. 4.36
w = corner deflection, in inches, which was determined from Eq. 4.16 based on a 9000-lb (40-kN) load with a contact pressure of 90 psi (621 kPa) applied at a free corner
FI = mean air freezing index, in degree days
B = erodibility factor for subbase materials: 0.5 for lean concrete subbase, 1.0 for cement-treated granular subbase, 1.5 for cement-treated nongranular subbase, 2.0 for asphalt-treated subbase, 2.5 for untreated granular subbase
ES = edge support condition: 0 for no edge support, 1 for tied edge beam or tied concrete shoulder
S = subgrade soil type: 0 for A-4 to A-7, 1 for A-1 to A-3
D = drainage index, with 0 for no edge drains and 1 for edge drains

Figure 12.6 is a plot of predicted faulting versus observed faulting for these 186 sections of undoweled pavements. Note that Eqs. 12.4 and 9.54*b* are of the same form and contain the same variables, but the regression constants are completely different and due to the scope of the data base.

Table 12.1 shows a sensitivity analysis of faulting in undoweled pavements based on Eq. 12.4. The parameter values shown in column 2 are used as the standard case. In the other seven cases, only the parameter shown in column 1 is changed in value from column 2 to column 3, while the other values remain the same as in column 2. For each case, the amount of faulting and its ratio to the standard case are tabulated.

A review of Table 12.1 indicates that, unless the freezing index is extremely high, edge support and the joint opening, which are directly related to the load transfer across the joint and edge, have the most effect on faulting and that corner deflection, which is related to slab thickness, is not very sensitive to faulting.

12.1.5 Joint Deterioration

Joint deterioration includes spalling and general breakup of the concrete near the joints. No mechanistic methods have been developed to analyze joint deterioration.

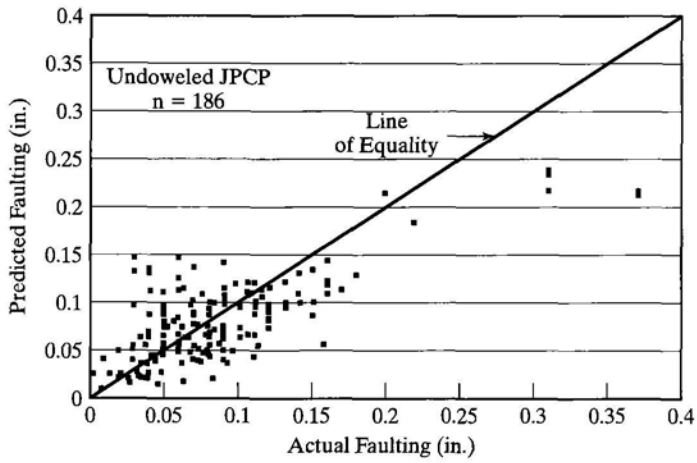

FIGURE 12.6

Predicted faulting versus observed faulting for undoweled pavements (1 in. = 25.4 mm). (After NCHRP (1990).)

TABLE 12.1 Sensitivity Analysis of Undoweled Pavements

Case	Change		Faulting	
	From	To	in.	Ratio
(1)	(2)	(3)	(4)	(5)
Standard case			0.118	1.00
ESAL, N_{18} (10^6)	10	20	0.147	1.25
Joint opening z (in.)	0.04	0.08	0.180	1.53
Corner deflection w (in.)	0.01	0.04	0.131	1.11
Freezing index FI (degree-days)	100	2000	0.268	2.27
Edge support ES	0	1	0.043	0.36
Base erodibility B	2.5	0.5	0.099	0.84
Subgrade soil type S	0	1	0.095	0.81
Drainage index D	0	1	0.098	0.83

Note. 1 in. = 25.4 mm.

The most important factor that causes joint deterioration is the "D" cracking of concrete, as described in Section 9.1.2. Therefore, the use of aggregates that do not cause "D" cracking is the first requisite to prevent joint deterioration.

A statistically based model was developed using the COPES data base. All pavements showing "D" cracking and reactive aggregate distress were removed from the data base, and nonlinear regression techniques were used on the remaining pavement sections. With over 501 pavement sections around the country, the following regression equation was obtained:

$$\text{DETJT} = (\text{AGE})^{2.3503}(N_{18})^{0.62974}\,[-0.0021443 + 3.6239 \times 10^{-6}\,(\text{FI}) + 7.08597 \times 10^{-5}\,(\text{JS}) + 3.5307 \times 10^{-5}\,(\text{SCTE})] \tag{12.5}$$

In this equation,

DETJT = percentage of deteriorated joints
AGE = time in years since construction started
N_{18} = number of 18-kip equivalent single-axle loads, in millions
FI = mean air freezing index, in degree days
JS = transverse joint spacing, in ft
SCTE = Thornthwaite summer concentration of thermal energy

Table 12.2 shows a sensitivity analysis of Eq. 12.5. It can be seen that age and joint spacing have the most effect on joint deterioration, the summer concentration of thermal energy the least effect.

12.1.6 Punchout Models

Punchouts are the primary mode of distress in CRCP, as described in Section 9.1.2. If this type of distress could be eliminated, CRCP would have an outstanding performance record. A comprehensive study was made by Zollinger (1989) on punchout distress. He described four modes of distress that eventually lead to punchout, as illustrated in Figure 12.7.

When the concrete slab cracks, the tensile stress in the steel reinforcement causes the fracture of surrounding concrete, as shown in (*a*). The fracture of concrete reduces the stiffness of the slab and results in spalling on the crack surface, as shown in (*b*). The spalling on the crack surface makes the crack open wide and results in the loss of load transfer across the crack, as shown in (*c*). Without the load transfer, the slab between two cracks acts as a cantilever beam, and the tensile stress in the transverse direction due to the edge loading causes the slab to crack at the top, as shown in (*d*).

Figure 12.8 shows the stresses at two critical locations in a CRCP under an 18-kip (80-kN) single-axle load. The stresses are presented in terms of load transfer efficiency (LTE) and crack spacing. Based on the analysis by ILLI-SLAB, the figure shows that the maximum longitudinal tensile stress σ_B at the bottom of the slab is highly sensitive to crack spacing but is relatively unaffected by LTE across the crack. The transverse tensile stress σ_A on the top of the slab is highly sensitive to LTE whenever the crack

TABLE 12.2 Sensitivity Analysis of Joint Deterioration

	Change		Joint deterioration	
Case	From	To	%	Ratio
(1)	(2)	(3)	(4)	(5)
Standard case			7.426	1.00
AGE (year)	10	30	98.209	13.23
ESAL N_{18} (10^6)	10	30	14.833	2.00
FI (degree-day)	100	2000	14.002	1.89
JS (ft)	100	15	1.674	0.23
SCTE	70	35	6.246	0.84

Note. 1 ft = 0.305 m.

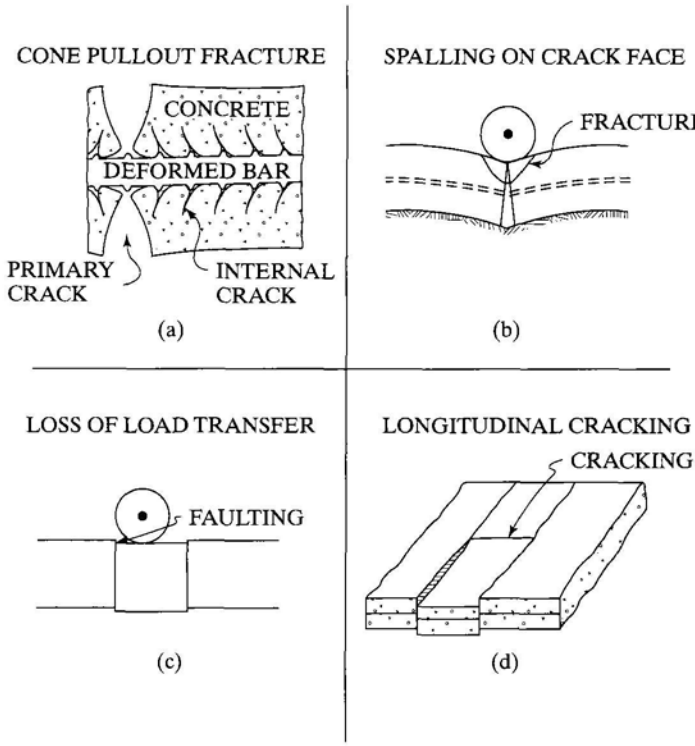

FIGURE 12.7

Failure modes leading to punchout distress. (After Zollinger and Barenberg (1990).)

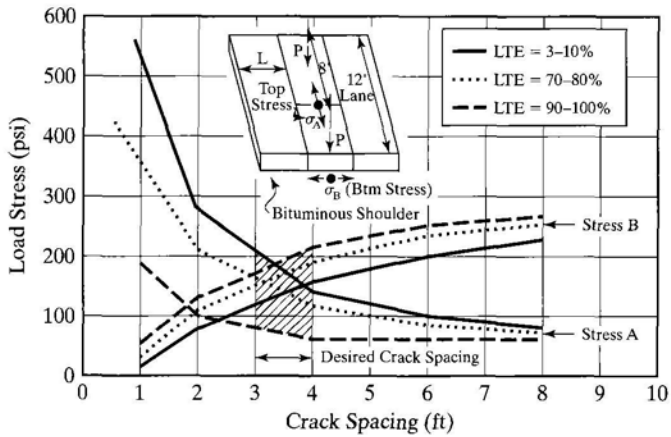

FIGURE 12.8

Comparison of σ_A and σ_B in CRCP for a 10-in. slab (1 psi = 6.9 kPa, 1 ft = 0.305 m). (After Zollinger and Barenberg (1990).)

spacing is less than 4 ft. These results indicate that, if the LTE can be maintained above 90%, the maximum transverse stress will remain relatively low even when the crack spacing is small. When the LTE drops to 70% or lower, the maximum transverse stress becomes increasingly large as the LTE and crack spacing decrease. When the tensile stress exceeds the tensile strength, a longitudinal crack will occur. The combination of

poor load transfer, voids around the reinforcing steel, longitudinal cracks, and so on, results in a punchout.

A mechanistic method of design to prevent punchout requires a knowledge of LTE, which depends on the level of shear stress across the crack and the crack width. The level of shear stress can be obtained from the finite element computer programs, but the determination of crack width requires an accurate prediction of crack spacing. Under normal construction conditions, crack spacings vary so widely that a reliable design procedure cannot be achieved. For the design approach to be reliable, some means of external control on the crack spacing is needed.

12.2 PORTLAND CEMENT ASSOCIATION METHOD

The Portland Cement Association's (PCA) thickness-design procedure for concrete highways and streets was published in 1984, superseding that published in 1966. The procedure can be applied to JPCP, JRCP, and CRCP. A finite element computer program called JSLAB (Tayabji and Colley, 1986) was employed to compute the critical stresses and deflections, which were then used in conjunction with some design criteria to develop the design tables and charts. The design criteria are based on general pavement design, performance, and research experience, including relationships to performance of pavements in the AASHO Road Test and to studies of pavement faulting. Design problems can be worked out by hand with tables and charts presented herein or by a microcomputer program available from PCA.

12.2.1 Design Criteria

One aspect of the new design procedure is the inclusion of an erosion analysis, in addition to the fatigue analysis. Fatigue analysis recognizes that pavements can fail by fatigue of concrete; in erosion analysis, pavements fail by pumping, erosion of foundation, and joint faulting.

Fatigue Analysis Fatigue analysis is based on the edge stress midway between the transverse joints, with the most critical loading position being shown in Figure 12.9. Because the load is near the midslab far away from the joints, the presence of the joints has practically no effect on the edge stress. When a concrete shoulder is tied onto the mainline pavement, the magnitude of the critical stress is reduced considerably.

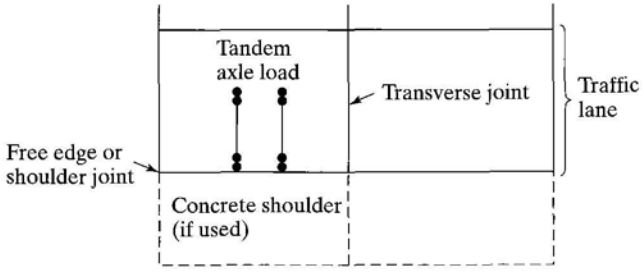

FIGURE 12.9
Critical loading position for fatigue analysis.